Aluminium distribution in ZSM-5 revisited: the role of Al-Al interactions

Article

Accepted Version

Ruiz-Salvadora, A.R., Grau-Crespo, R. ORCID: https://orcid.org/0000-0001-8845-1719, Gray, A. E. and Lewis, D. W. (2013) Aluminium distribution in ZSM-5 revisited: the role of Al-Al interactions. Journal of Solid State Chemistry, 198. pp. 330-336. ISSN 0022-4596 doi: https://doi.org/10.1016/j.jssc.2012.10.022 Available at https://centaur.reading.ac.uk/36086/

To link to this article DOI: http://dx.doi.org/10.1016/j.jssc.2012.10.022

Publisher: Elsevier

Aluminium distribution in ZSM-5 revisited: the role of Al-Al interactions

A. Rabdel Ruiz-Salvador[a*], Ricardo Grau-Crespo[b], Aileen E. Gray[b] and Dewi W. Lewis[b]

[a] *Group of Materials Developed by Design, Division of Chemistry and Technology of Materials, Institute of Materials Science and Engineering (IMRE), University of Havana, Havana 10400, Cuba. E-mail: rabdel@imre.oc.uh.cu*

[b] *Department of Chemistry, University College London, 20 Gordon Street, London, WC1H OAJ, UK.*

Corresponding Author:
Dr. A. Rabdel Ruiz-Salvador
Group of Materials Developed by Design
Division of Chemistry and Technology of Materials
Institute of Materials Science and Engineering (IMRE)
University of Havana, Havana 10400, Cuba.
E-mail: rabdel@imre.oc.uh.cu
Phone: (537)-8790308
FAX: (537)-8794651

Abstract

We present a theoretical study of the distribution of Al atoms in zeolite ZSM-5 with Si/Al=47, where we focus on the role of Al-Al interactions rather than on the energetics of Al/Si substitutions at individual sites. Using interatomic potential methods, we evaluate the energies of the full set of symmetrically independent configurations of Al siting in a $Si_{94}Al_2O_{192}$ cell. The equilibrium Al distribution is determined by the interplay of two factors: the energetics of the Al/Si substitution at an individual site, which tends to populate particular T sites (e.g. the T14 site), and the Al-Al interaction, which at this Si/Al maximises Al-Al distances in agreement with Dempsey's rule. However, it is found that the interaction energy changes approximately as the inverse of the square of the distance between the two Al atoms, rather than the inverse of the distance expected if this were merely charge repulsion. Moreover, we find that the anisotropic nature of the framework density plays an important role in determining the magnitude of the interactions, which are not simply dependent on Al-Al distances.

Keywords: MFI, ZSM-5, site disorder, cation distribution, interatomic potentials

1 Introduction

Most of the exploited properties of microporous aluminosilicates, typified by zeolites, are connected to the presence of Al atoms in the framework. The charge unbalance introduced in an otherwise all-silica framework can be compensated either with protons, resulting in (catalytically active) Brønsted acidity, or with (exchangeable) extra-framework cations, Lewis acidity and molecular adsorption and separation properties [1]. Pioneering work by Lowenstein [2] and Dempsey et al. [3] established simple qualitative rules describing likely Si-Al distribution in zeolites: according to Lowenstein's rule, Al-O-Al links are unlikely in zeolites, while Dempsey generalized this principle to state that Al ions tend to locate as far as possible from each other in the framework for a given Si/Al ratio. These rules can be rationalised in terms of energetic (thermodynamic) considerations, as has been widely shown using computer simulation methods [4], although the validity of Dempsey's rule has been questioned for some zeolites [5]. It is also clear that kinetic factors also influence the cation distribution, especially at high Si/Al ratios. But an understanding of the thermodynamic factors affecting the cation distribution still provides valuable insight that can, for example, allow the determination of optimal compositions and an improved representation of the chemical processes occurring in these materials.

Computational chemistry methods have a long established role in zeolite chemistry. However, the construction of realistic models of the cation distribution in a zeolite for a computational study can be time-consuming and if not done with sufficient care it may influence (incorrectly) the computed properties. While the Lowenstein and Dempsey rules are of help, it would be useful to have a more quantitative framework to allow the creation of meaningful models, using for example rapid energy evaluations within a Monte Carlo approach. Our main goal here is to obtain a quantitative description of the effect of Al-Al interactions in the cation distribution for a zeolite with a relatively high Si/Al ratio, notwithstanding the self-assembly processes. These quantitative rules will allow us to construct suitable models for further study.

Zeolite ZSM-5 (MFI framework) is one of the most versatile and widely used materials in the field of heterogeneous catalysis, with remarkable applications in petrochemical processes, e.g. xylene isomerisation, oil dewaxing and methanol-to-gasoline conversion, as well as in fine chemistry and pollution control [6]. Its exceptional catalytic properties are due to a peculiar 3-dimensional 10-ring channel system consisting of intersecting straight and sinusoidal channels (Figure 1). Since the connectivity of the channels in the [001] direction is through the sinusoidal channel, the overall 3-dimensional motion is rather slow. In addition, the confinement field acting on the molecules is particularly intense due to the medium size of the cavities (ca. 5.5 Å) which leads to strong molecular interactions with the active sites.

The topic of Al distribution in ZSM-5 has stimulated a significant amount of research using both experimental [7] and theoretical techniques [8]. There is some evidence that the synthesis conditions and (random) self-assembly processes significantly affect the Al distribution in ZSM-5, particularly at high Si/Al. Nevertheless, there are few analyses of the experimental and computed distributions that establish any guides to the construction of model material for computational study. Moreover, few of the above studies consider the factors that result in unlikely distributions (beyond the non-Lowensteinian behaviour).

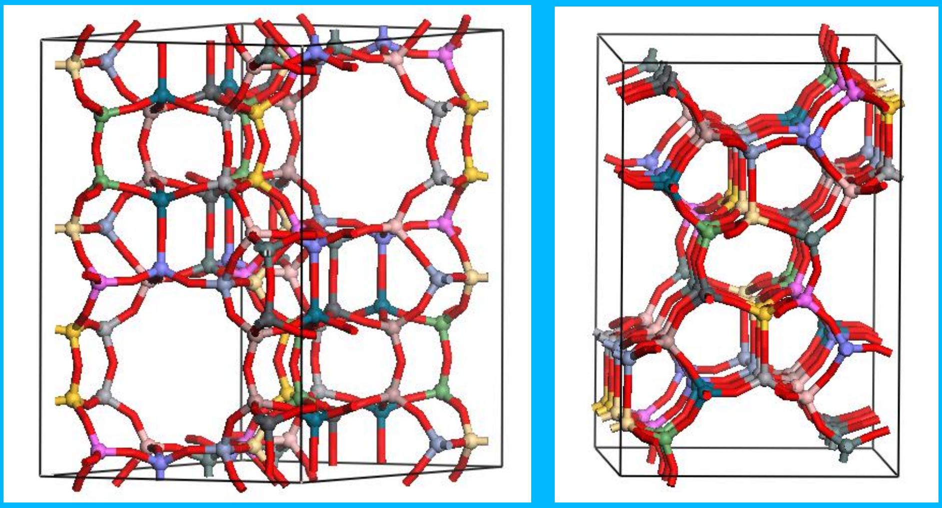

Figure 1. The ZSM-5 unit cell, showing the sinusoidal channel (parallel to [100]) and the straight channel (parallel to [010]) of the zeolite. The distinct 12 T sites of the orthorhombic cell are shown with balls of different colours, oxygen atoms are depicted by red sticks.

The unit cell of ZSM-5 has 96 tetrahedral (T) sites occupied by either Si or Al. There are 12 symmetrically unique T sites (Figure 1) when described in the orthorhombic Pnma space group, which the structure adopts at temperatures above ~340 K [9] whilst the number is doubled to 24 in the low-temperature monoclinic structure ($P2_1/n11$ space group) [10]. Diffraction methods provide little information on Si/Al distributions, as they can only detect a very large Al occupancy of a particular site, which is unlikely to be the case for the high Si/Al ratios commonly typically found in MFI. For example, Lermer et al. have studied MFI samples with Si/Al ~ 12 using diffraction techniques, but the large standard errors obtained for the T-O distances prevented the analysis of the sites occupancies [11]. Vezzalini et al. have suggested, based on diffraction studies, that the Si/Al distribution remains disordered in the low Si/Al (7.6) natural analogue mutinaite [12], while Olson et al. have suggested non-random aluminium distribution based on the location of charge-compensating caesium ions, using both diffraction techniques and computational modelling [7e].

NMR studies also appear to provide contradictory indicators of siting and order. For example, whilst Sarv et al. found random distribution of Al over the framework [7d], non-random distribution was later suggested by Han et al [7f]. In addition to NMR, other spectroscopic techniques have been also employed. For example, Dedecek, Witcherlova and co-workers have used UV-Vis-NIR to study the Al distribution in MFI, under the assumption that divalent extra-framework cations can be used as probe to monitoring the Al location [7a,b]. They have concluded that the Al distribution is not random, but depends on the chemical composition of the zeolite and on the synthesis conditions, a result that has been confirmed by more recent studies using NMR and theoretical calculations [8l,m].

Most theoretical studies focused on Al siting in MFI zeolites have been conducted by comparing the energies of configurations including Al and charge compensating neighbouring protons [8a-h]. However, this approach is not consistent with the fact that, during synthesis, Al ions are first located in the framework in the absence of protons, which are incorporated in their final positions only later, after the calcination step, when the Al distribution is not expected to change. We also noted that using protons as charge compensation in a theoretical study has an additional drawback associated to the large local stress (not present during the synthesis) introduced by the 0.1Å enlargement of the T-O distances upon H^+ siting on the Al-Si bridging oxygen. This shift of the T-O distances is of the same magnitude of the difference between Al-O and Si-O distances, then it is expected that calculations based on protons as compensating charges should carry an artificial large stress. Therefore, when investigating the energetics of Al distribution in a zeolite, it is important to choose a different charge compensating mechanism, instead of protons. Ideally, one would like to simulate the Al-distribution in a model of the as-synthesised zeolite, including water, template molecules and extra-framework cation species, but the consideration of these effects, even in the simplest approximations, is computationally demanding [13]. At such high Si/Al the counterions are typically organic templates, where the charge is distributed over the molecule. Thus, as discussed further below, we do not consider the template explicitly: inclusion of which would introduce errors in the location of the template, the charges used and the compatibility of an ionic zeolite model and a molecular mechanics description of the organic.

In ref. [8k] we introduced a methodology to study the incorporation of the Al atoms and protons in two steps: the distribution of Al was first determined in the absence of protons, which are incorporated in a second step around the most stable Al positions. Thus, we study here the Al distribution without dealing with the proton distribution, expanding the study to the case of 2 Al per unit cell, which will allow a better understanding of the role of the Al-Al defect interaction on the distribution.

2 Methodology

All calculations were performed using GULP (General Utility Lattice Program) code [14], which allows the use of a wide range of interatomic potential functions for the simulation of solids. Whereas first-principles periodic calculations have been employed for the study of heteroatom location in zeolites [15], in the present paper we have chosen to use forcefield calculations due to the large set of configurations to be analysed. Such interatomic potential descriptions have been widely applied in the study of zeolites, owing to its good balance between accuracy and computational cost [4,16] and have been shown to be in excellent agreement with experimental work in terms of both geometries and thermodynamic properties. [13a,17]. In previous works we have rigorously validated, against experimental crystallographic results, the use of interatomic potentials for the study of the Si-Al distribution in zeolites [13a,13e,18].

The widely used potentials by Sanders et al. [19], with the Jackson and Catlow modifications [20], were employed to model the interactions in the zeolite framework. Short-range interactions are handled in real space within a cut-off distance (16Å), while the slowly convergent long-range interactions are calculated using the Ewald’s summation method [21]. Both the cell parameters and the ionic positions were relaxed for each configuration. A convergence criterion for the forces of 0.001 eV/Å was used. The relaxation starts with the Newton-Raphson minimiser, updating the Hessian matrix by the BFGS approximation [22], and after reaching a suitable value of the gradients' norm it switches to the RFO minimiser [23]. This procedure ensures convergence to real minima, i.e. with no imaginary modes, a fact of particular relevance when dealing with zeolitic materials [24].

For the lattice energy calculations the neutrality of the cell was maintained by uniformly smearing a compensation charge over all framework oxygen atoms, avoiding the necessity of explicit extra-framework species. This is clearly an approximation, since in the as-synthesized zeolite the charge is compensated by typically organic templates, particularly in high silica system, as the extra-framework species. However, it is known that this extra-framework charge is rather delocalised over the templates' atoms [25]. If templates were to be considered, we would have to compute charges using quantum methods, introducing uncertainty and also since the charges used on the framework are formal, the mismatch between the organic and inorganic components will introduce further uncertainly. Moreover, we must ensure that the location of the template is determined accurately, were there is little experimental (apart from the exemplar tetraproplyammonium) corroboration. In absent of such *a priori* structural data on the location of the extra-framework cations (either organic or metal cations), one would need to computationally explore for each given Si-Al distribution a range of possible cations distributions [18c]. This would be, as stated above, an extremely expensive route that rules out a wide scan of Si-Al distribution study.

We therefore assume that the stability of the Al substitution, at such high Si/Al ratio, is not significantly affected by the exact position of the extra-framework cation and implicitly include the charge compensation by smearing the charge on the framework. Note that since we have as many as 192 O atoms per cell, the compensation correction introduced on each oxygen charge is sufficiently small to not alter the T-O and O-O interactions. We have confirmed (see next section) that the present procedure, when applied to the case of one Al Atom per unit cell (oxygen charges change from -2.0 to -1.9948, a correction of 0.26%), yields results which are in good agreement with those obtained by using the Mott-Littleton methodology, as calculated in ref. [8c,8k]. Here, when two Al atoms are considered, the oxygen charge is now corrected to -1.9896. Note that in this case the charge reduction is still very small (0.52% of the nominal value). An approach similar to this one was used by Kramer and van Santen, but the charge imbalance was compensated by varying the charge of the Si atoms [26].

We optimised all the 1176 different Si-Al configurations in the unit cell with composition $Si_{94}Al_2O_{192}$. The search for the inequivalent configurations was carried out by exploiting the lattice symmetry, following the methodology developed by Grau-Crespo et al [27]. Two substitutional configurations are considered equivalent if they are related by a symmetry operator of the parent (non-substituted) structure. It is then possible to discuss the ion distribution using Boltzmann statistics: the probability of occurrence of a given independent configuration m, with energy E_m and degeneracy Ω_m (the number of times it appears in the full configurational space), is given by:

$$P_m = \frac{\Omega_m}{Z} \exp(-E_m / RT) \qquad (1)$$

where Z is the partition sum, which guarantees that the sum of all the probabilities equals one; R is the gas constant, and T is the equilibration temperature for the cation distribution, which in the case of zeolites is often assumed to correspond to the synthesis temperature (typically around 150 °C) [8c,8k]. Symmetry-adapted Boltzmann ensembles have been employed for the study of ion disorder in a wide range of materials including mixed oxides [28], sulphides [29], carbonates [30] and hydrides [31].

3 Results and discussion

The lattice energies of the unit cells containing 1 Al atom per unit cell (Si/Al= 95) are first calculated in order to obtain the probabilities for isolated occupancies of different sites, and to compare the results using periodic calculations with those obtained in the limit of isolated substitutions. The relative lattice energies of the 24 different structures calculated by means of the smeared charges are showed in Figure 2, in comparison with the relative defect energies of the Si-Al substitution as calculated previously in Ref [8k] by the Mott-Littleton methodology (Si/Al= infinity, as an Al atom is introduced as an isolated defect). The differences are small, and are mainly due to the deformation of the unit cells arisen from the presence of Al atoms and also to the interactions between Al atoms of neighbouring cells, both factors presented in the periodic calculations but absent in the Mott-Littleton study. As the unit cell is large, Al-Al interactions arising from the periodicity of the system are expected to be small, which is supported by the correlation shown in Fig. 2. Both the periodic and the Mott-Littleton calculations indicate that the T14 site, which is located in the sinusoidal channel of the zeolite, is the most favourable position for Al substitution.

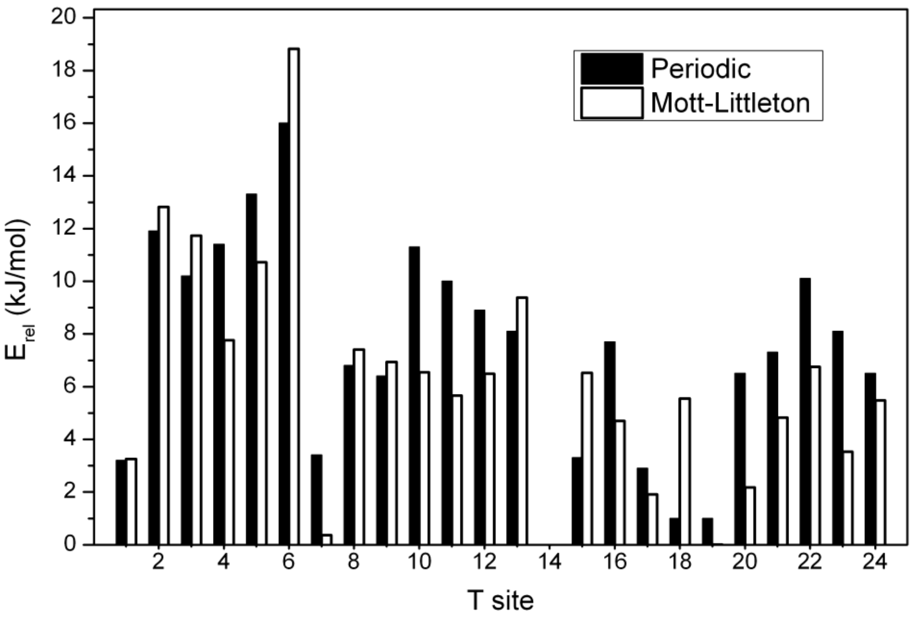

Figure 2. Relative lattice energies of the 24 symmetrically independent configurations of 1-Al per unit cell (solid bars), in comparison with the Mott-Littleton defect energies calculated in Ref. [8k] (open bars). Energies are relative to those for T14, the most stable site for isolated substitution by both methods.

Now we consider the case of two Al substitutions per cell. The variation in the relative positions of the Al ions leads to a dependence of the substitution energy of the form:

$$E_{ij} = E_i + E_j + \Delta E_{ij} \tag{2}$$

where E_{ij} is the energy of the configuration with Al ions substituted in sites i and j, E_i and E_j are the energies of the configurations with one Al ion substituted in sites i and j, respectively (all these energies are given with respect to the non-substituted, pure Si zeolite), and ΔE_{ij} is interaction energy between Al ions when they are located at these sites. Thus, if the two substitutions were not interacting, a plot of the two-Al energies versus the sum of the corresponding one-Al energies should give a slope of 1. Many configurations do indeed lie near the slope = 1 line, as shown Fig. 3, but the plot exhibits significant scattering, which is a clear indication that even at this relatively high Si/Al ratio (= 47) the interaction effects could have a controlling effect on the Al distribution. As expected, the highest-energy configurations (above 100 kJmol^{-1}) are non-Lowensteinian structures, that is, those exhibiting Al-O-Al links.

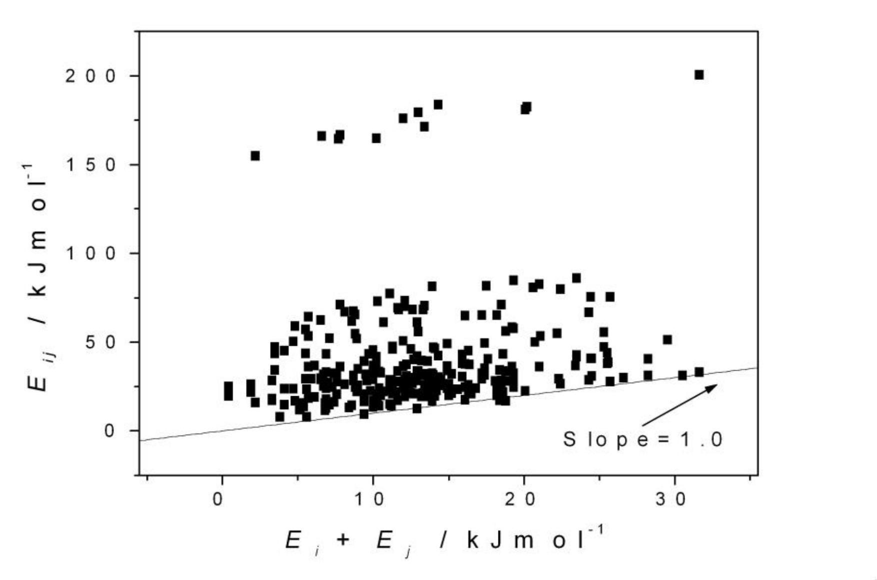

Figure 3. Energy of 2Al configurations as a function of the sum of the isolated 1Al containing ZSM-5. Points at the top of the figure corresponds to non-Lowensteinian configurations.

It is illustrative to discuss the trend in the relative energies in terms of Boltzmann probabilities. Figure 3 implicitly indicates that the location of Al atoms is biased towards the preferential sites at single Al atom occupation, since the product of the probabilities of finding Al atoms at these sites (P_1 P_2) is proportional to the negative exponential of the sum of their energies ($\exp(-(E_1+ E_2)/kT)$. In the absence of Al-Al interactions the probability of each two-Al pair (P_{12}) would be equal to the product of the single probabilities (P_1 P_2). The presence of the positive interaction term then decreases the probability of occurrence of a given configuration with respect to what it would be in the absence of interactions.

We now consider what geometric features influence the magnitude of the Al-Al interactions. The magnitude of the interaction depends on the relative position of the Al atoms; the direct Al-Al distance can be expected to be the most important factor. Note that each Al atom will be surrounded by 6 replicas of itself in the nearest neighbour cells, whose interatomic distances will not vary significantly from one Si-Al distribution to another. Therefore, when comparing Al-Al distances we refer to the closest distinct Al-Al distance, but keep in mind that a nearly constant contribution from the translational symmetry is also present.

The plot of the interaction energy ΔE versus the minimum distinct Al-Al distance in the structure is shown in Figure 4a. We have used the distances between the T-sites as they appear in a relaxed Al-free structure (see explanation below). A clear correlation is found in Figure 4a, showing a decrement of the interaction energy with the Al – Al distance. We have fitted this data to power laws of the type $\Delta E \sim d^{-n}$ for different positive and integer n values and find the optimal fit with n=2 with the average quadratic deviation from the fitting function χ^2 =43.9, far better than for n=3 (χ^2 =61.9) and n=1 (χ^2 =102.2). Allowing the exponent n to take non-integer values yields n=2.18, but with little improvement in the goodness of fit (χ^2 =42.8). Thus, we can state, to a good approximation, the interaction energy decreases with the square of the Al-Al distance. The observation that a better fit is obtained for a $\sim d^{-2}$ dependence rather than d^{-1}, suggests that the interactions are not simply dominated by the direct Al-Al electrostatic repulsion. Other factors, like the propagation of short-range forces, or the overlap of local distortions, must be significantly affecting the interaction energy. We note that Sastre et al observed that the distortions of the local geometry are an important factor in the location of a single Al atom [32].

As mentioned above, the distances used to construct Figure 4 are those from the host (relaxed) silicalite structure rather than from the actual 2-Al structures. Our reasoning for this is two-fold: (i) the silicalite structure provides a common reference for all structures, and (ii) more importantly, the calculated energies represent a measure of the deformation of the crystal from the pure silica framework (a given reference) due to the Al incorporation. In fact, the correlations obtained are slightly better (by ca. 10% in the χ^2 values) when analysed in this way, compared to using the final relaxed distances.

Even though the d^{-2} correlation is strong, the dispersion in the interaction energy as a function of Al-Al distance suggests that shielding of the interaction by the pore walls is clearly important and we now consider how the anisotropy of the structure may be playing a role here. The well-defined channels in MFI are along the x and y axes and not in z. Hence, the xy plane is more dense and rigid than the other (more flexible) planes xz and yz, and thus distortions in the xy plane are expected to be more energetically costly. Indeed, our results support this view (Figure 4 b, c and d) as the d^{-2} correlation is strongest in the xy component (d_{xy}) of the Al – Al distance, but less so with the xz and yz components.

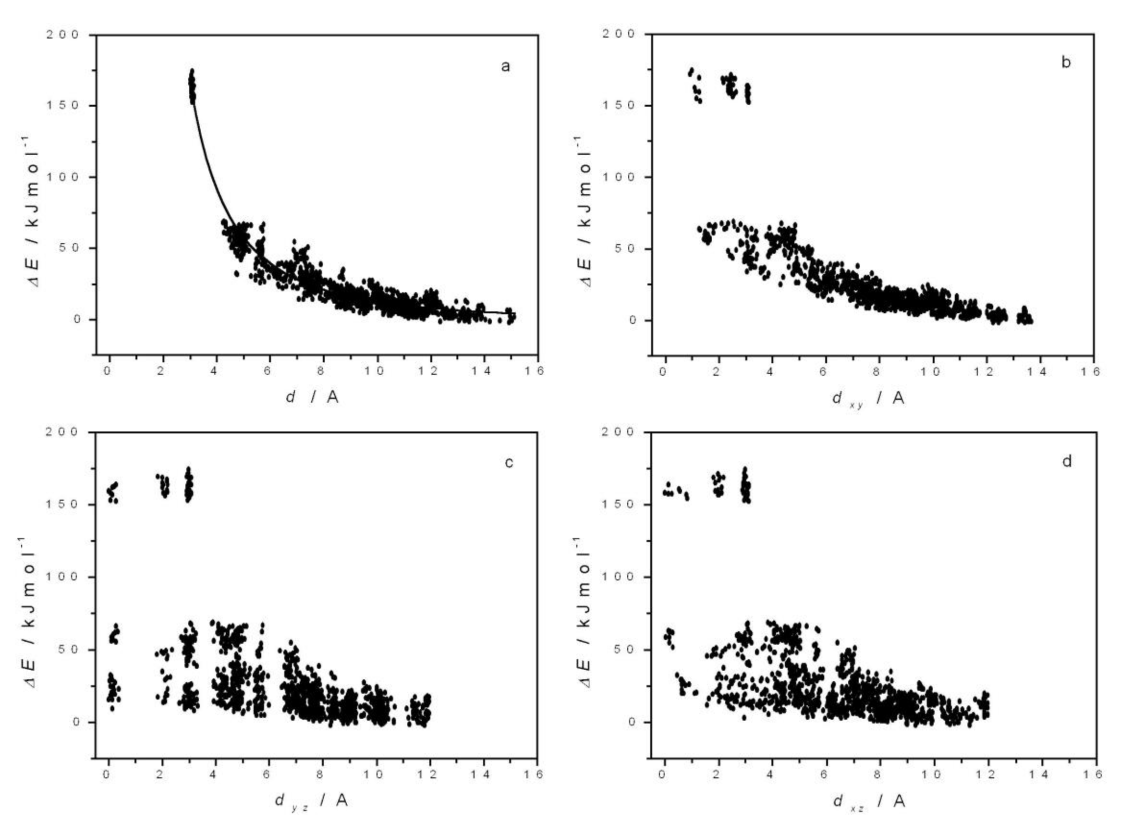

Figure 4. Dependence of the interaction energy with the Al-Al distance, (4a), and with the projection of this distance on the planes xy (4b), yz (4c) and xz (4d).

The general trend in the energetics of the configurations is in agreement with Dempsey's rule [3]. However, the dispersion observed in Figure 4a, i.e. the existence of different values of energies for similar Al-Al distances, indicates that the rule cannot be applied unambiguously, even at such high Si/Al. This dispersion is not related to the preferential occupancy of certain types of sites in the zeolite, because this effect was already subtracted from the interaction energy following the equation (2). It is most likely related to the anisotropy of the lattice. For example consider the dispersion for configurations with *d*(Al-Al) just below 6Å: the dispersion width is almost 50 kJ mol^{-1} in the *yz* and *xz* planes, but less than half of this in the *xy* plane (Figure 4).

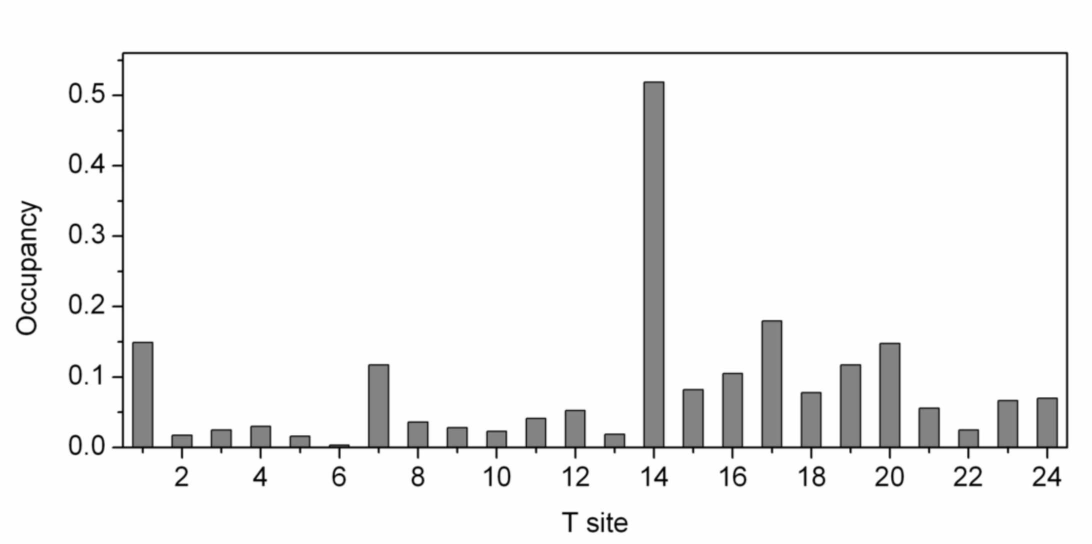

Figure 5. Estimated Al occupancy factors for each of the 24 symmetrically distinct sites, for MFI with Si/Al=47, at a typical synthesis temperature (150 ^{o}C). The sum of all the occupancies equals 2.

The equilibrium Al distribution then results from the interplay between two factors: the individual site preference and the interaction between impurities. The effect of the former is clear if we look at the estimated occupancies of the different sites (figure 5), which were calculated based on the Boltzmann probabilities assuming a typical synthesis temperature (150 ^{o}C). The T14 site, which is the most stable site when only one Al is considered, is by far the highest populated, with around 50%-50% Si/Al composition. Furthermore, eight out of the twelve most stable configurations in the ensemble have at least one Al atom in a T14 position, as shown in Table 1. The global energy minimum for this composition (recall we have considered all possible configurations) is a configuration where both Al ions are in T14 sites. This analysis indicates that, at least for this Si/Al, individual site preference is still the strongest factor in the Al distribution. However, the role of the Al-Al interaction in determining the distribution is also obvious from Table 1: all the most stable configurations have Al-Al distances greater than 10 Å. While substitution at T14/T19 should be more stable than substitution at T14/T20 based only on individual sites preferences (T19 has a lower substitution energy than T20), the opposite happens, because the T14-T20 distance is longer than the T14-T19 distance. The energy differences introduced by interaction effects are significant, because the exponential nature of Boltzmann's distribution means that the probability of occurrence decays very rapidly with the configuration energy (figure 6).

Table 1. Twelve 2-Al configurations with the highest occurrence probabilities: Configuration labels represent the distinct T site with the group symmetry operation in parenthesis, P_1 and P_2 stand for the probability of finding a single Al atom, *d*(Al-Al) is the shortest Al-Al distance, Ω is the degeneracy of the configuration, and *P* is its probability of occurrence.

Configuration	P_1	P_2	*d*(Al-Al)[Å]	E_{rel}[kJMol^{-1}]	Ω	*P*
14(1); 14(4)	0.0353	0.0353	13.3941	0	2	0.0453
14(1); 20(4)	0.0353	0.0190	12.7938	4.4737	4	0.0127
14(1); 19(4)	0.0353	0.0352	10.4076	6.1171	4	0.0079
1(1); 17(2)	0.0140	0.0205	13.3635	6.3217	4	0.0075
17(1); 17(4)	0.0205	0.0205	13.3625	7.2792	4	0.0057
14(1); 15(4)	0.0353	0.0055	13.2125	7.3246	4	0.0056
17(1); 17(3)	0.0205	0.0205	13.3618	7.7868	4	0.0049
14(1); 18(4)	0.0353	0.0073	10.9811	7.8664	4	0.0048
1(1); 14(2)	0.0140	0.0353	12.5375	7.8863	4	0.0048
1(1); 1(4)	0.0140	0.0140	12.7429	7.9749	4	0.0047
14(1); 16(4)	0.0353	0.0093	11.0862	8.3769	4	0.0042
14(1); 21(4)	0.0353	0.0089	12.5967	8.4111	4	0.0041

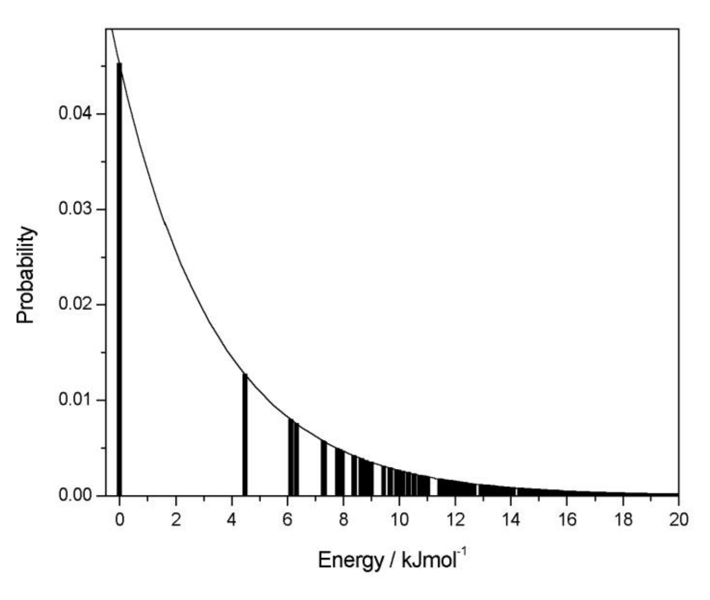

Figure 6. Dependence of the occurrence probabilities of 2-Al configurations on their energies at T=423 K.

Before finishing the discussion, it is worth to remember that the results shown here have been obtained using a model that does not contain extra-framework charge compensating cations. However, in a typical synthesis the presence of charged organic templates besides a structure directing role might have an impact in the Al location [32-33]. In the case of ZSM-5 prepared with quaternary ammonium ions, as usually, the Al-location controlling role is expected to be less relevant due to the shielding effect of the organic substituents, as shown for the pentasil zeolite FER by Gomez- Hortiguela et al. [33b].It is then expected that the main features with regards the Si-Al distribution in high silica (Si/Al = 47) ZSM-5 and the effect of the Al – Al interactions on this issue have been well captured in this study.

4. Conclusions

In the light of our results we conclude that Al-Al interaction in zeolites is a key factor in controlling Si-Al distribution, even at relatively high Si/Al. Such interactions will clearly become even more important at lower Si/Al, where we expect Dempsey's rule to be less relevant, as we have shown in previous work [18a,b]. The local geometry will control the inclusion of dilute Al impurities, but Al-Al interactions become increasingly important as more Al is incorporated.

The overall dependence of the interaction energies with the Al-Al distances indicates that the general trends in the location of the Al atoms is to maximize their relative distances, describing a Dempsey-like behaviour. We have given a more quantitative form to this principle, by showing that the Al-Al interaction energy changes in inverse proportion to the square of the Al-Al distance d. This behaviour suggests that Coulomb interactions are not the main contribution to the energy differences. Moreover, we find a strong dependence on the density of the framework, particularly within the xy plane. To the best of our knowledge this is the first time that the anisotropy of the framework is identified as a source of departure from Dempsey's rule at such high Si/Al ratios.

Acknowledgments

Partial support from the University of Havana and UCL are grateful acknowledged.

References

Table 1. Twelve 2-Al configurations with the highest occurrence probabilities: Configuration labels represent the distinct T site with the group symmetry operation in parenthesis, P_1 and P_2 stand for the probability of finding a single Al atom, *d*(Al-Al) is the shortest Al-Al distance, Ω is the degeneracy of the configuration, and *P* is its probability of occurrence.

Configuration	P_1	P_2	*d*(Al-Al)[Å]	E_{rel}[kJMol^{-1}]	Ω	*P*
14(1); 14(4)	0.0353	0.0353	13.3941	0	2	0.0453
14(1); 20(4)	0.0353	0.0190	12.7938	4.4737	4	0.0127
14(1); 19(4)	0.0353	0.0352	10.4076	6.1171	4	0.0079
1(1); 17(2)	0.0140	0.0205	13.3635	6.3217	4	0.0075
17(1); 17(4)	0.0205	0.0205	13.3625	7.2792	4	0.0057
14(1); 15(4)	0.0353	0.0055	13.2125	7.3246	4	0.0056
17(1); 17(3)	0.0205	0.0205	13.3618	7.7868	4	0.0049
14(1); 18(4)	0.0353	0.0073	10.9811	7.8664	4	0.0048
1(1); 14(2)	0.0140	0.0353	12.5375	7.8863	4	0.0048
1(1); 1(4)	0.0140	0.0140	12.7429	7.9749	4	0.0047
14(1); 16(4)	0.0353	0.0093	11.0862	8.3769	4	0.0042
14(1); 21(4)	0.0353	0.0089	12.5967	8.4111	4	0.0041

Figure Captions

Figure 1. The ZSM-5 unit cell, showing the sinusoidal channel (parallel to [100]) and the straight channel (parallel to [010]) of the zeolite. The distinct 12 T sites of the orthorhombic cell are shown with balls of different colours, oxygen atoms are depicted by red sticks.

Figure 2. Relative lattice energies of the 24 symmetrically independent configurations of 1-Al per unit cell (solid bars), in comparison with the Mott-Littleton defect energies calculated in Ref. [8k] (open bars). Energies are relative to those for T14, the most stable site for isolated substitution by both methods.

Figure 3. Energy of 2Al configurations as a function of the sum of the isolated 1Al containing ZSM-5. Points at the top of the figure correspond to non-Lowensteinian configurations.

Figure 4. Dependence of the interaction energy with the Al-Al distance, (4a), and with the projection of this distance on the planes xy (4b), yz (4c) and xz (4d).

Figure 5. Estimated Al occupancy factors for each of the 24 symmetrically distinct sites, for MFI with Si/Al=2, at a typical synthesis temperature (150 ^{o}C). The sum of all the occupancies equals 2.

Figure 6. Dependence of the occurrence probabilities of 2-Al configurations on their energies at T=423 K.

(1) (a) Breck, D. W. *Zeolite Molecular Sieves*; Wiley and Sons: New York, 1973(b) Davis, M. E. *Nature* **2002**, *417*, 813(c) *Introduction to zeolite science and pratice 3 Revised edition*; Cejka, J.; van Beekkum, H.; Corma, A.; Schuth, F., Eds.; Elsevier: Amsterdam, 2007; Vol. 168.
(2) Lowenstein, W. *Am. Miner.* **1954**, *39*, 92.
(3) Dempsey, E.; Kuhl, G. H.; Olson, D. H. *J. Phys. Chem.* **1969**, *73*, 387.
(4) *Modelling of Structure and Reactivity in Zeolites*; Catlow, C. R. A., Ed.; Academic Press: London, 1992.
(5) (a) Schroeder, K. P.; Sauer, J. *The Journal of Physical Chemistry* **1993**, *97*, 6579(b) Zokaie, M.; Olsbye, U.; Lillerud, K. P.; Swang, O. *Micropor. Mesopor. Mater.* **2012**, *158*, 175.

(6) (a) Venuto, P. B. *Studies in Surface Science and Catalysis* **1997**, *105*, 811(b) Stocker, M. *Microporous and Mesoporous Materials* **1999**, *29*, 46(c) Keil, F. J. *Microporous and Mesoporous Materials* **1999**, *29*, 49(d) de Angelis, A.; Ingallina, P.; Perego, C. *Industrial & Engineering Chemistry Research* **2004**, *43*, 1169 (e) Parvulescu, V. I.; Grange, P.; Delmon, B. *Catalysis Today* **1998**, *46*, 233(f) Degnan, T. F., Jr. *Studies in Surface Science and Catalysis* **2007**, *170*, 54.

(7) (a) Dedecek, J.; Kaucky, D.; Wichterlova, B. *Chemical Communications* **2001**, 970(b) Dedecek, J.; Kaucky, D.; Wichterlova, B.; Gonsiorova, O. *Physical Chemistry Chemical Physics* **2002**, *4*, 5406(c) Lin, J. C.; Chao, K. J.; Wang, Y. *Zeolites* **1991**, *11*, 376(d) Sarv, P.; Fernandez, C.; Amoureux, J. P.; Keskinen, K. *Journal of Physical Chemistry* **1996**, *100*, 19223(e) Olson, D. H.; Khosrovani, N.; Peters, A. W.; Toby, B. H. *Journal of Physical Chemistry B* **2000**, *104*, 4844(f) Han, O. H.; Kim, C. S.; Hong, S. B. *Angewandte Chemie-International Edition* **2002**, *41*, 469.

(8) (a) Derouane, E. G.; Fripiat, J. G. *Zeolites* **1985**, *5*, 165(b) Lonsinger, S. R.; Chakrabarty, D. K.; Theodorou, D. N.; Bell, A. T. *Catalysis Letters* **1991**, *11*, 209(c) Alvarado-Swaisgood, A. E.; Barr, M. K.; Hay, P. J.; Redondo, A. *Journal of Physical Chemistry* **1991**, *95*, 10031(d) Schroder, K. P.; Sauer, J. C.; Leslie, M.; Catlow, C. R. A. *Zeolites* **1992**, *12*, 20(e) Brand, H. V.; Curtiss, L. A.; Iton, L. E. *Journal of Physical Chemistry* **1992**, *96*, 7725(f) Brand, H. V.; Curtiss, L. A.; Iton, L. E. *Journal of Physical Chemistry* **1993**, *97*, 12773(g) Redondo, A.; Hay, P. J. *Journal of Physical Chemistry* **1993**, *97*, 11754(h) Blanco, F.; Urbinavillalba, G.; Deagudelo, M. M. R. *Molecular Simulation* **1995**, *14*, 165(i) Chatterjee, A.; Vetrivel, R. *Microporous Materials* **1994**, *3*, 211(j) Ricchiardi, G.; Newsam, J. M. *Journal of Physical Chemistry B* **1997**, *101*, 9943(k) Grau-Crespo, R.; Peralta, A. G.; Ruiz-Salvador, A. R.; Gomez, A.; Lopez-Cordero, R. *Physical Chemistry Chemical Physics* **2000**, *2*, 5716(l) Sklenak, S.; Dedecek, J.; Li, C.; Wichterlova, B.; Gabova, V.; Sierka, M.; Sauer, J. *Angewandte Chemie-International Edition in English* **2008**, *46*, 7286 (m) Sklenak, S.; Dedecek, J.; Li, C.; Wichterlova, B.; Gabova, V.; Sierka, M.; Sauer, J. *Physical Chemistry Chemical Physics* **2009**, *11*, 1237.

(9) Olson, D. H.; Kokotailo, G. T.; Lawton, S. L.; Meier, W. M. *Journal of Physical Chemistry* **1981**, *85*, 2238.

(10) Vankoningsveld, H.; Jansen, J. C.; Vanbekkum, H. *Zeolites* **1990**, *10*, 235.

(11) Lermer, H.; Draeger, M.; Steffen, J.; Unger, K. K. *Zeolites* **1985**, *5*, 131.

(12) Vezallini, G.; Quartieri, S.; Galli, E.; Alberti, A.; Cruciani, G.; Kvick, A. *Zeolites* **1997**, *19*, 323.

(13) (a) Almora-Barrios, N.; Gomez, A.; Ruiz-Salvador, A. R.; Mistry, M.; Lewis, D. W. *Chemical Communications* **2001**, 531(b) Sastre, G.; Leiva, S.; Sabater, M. J.; Gimenez, I.; Rey, F.; Valencia, S.; Corma, A. *Journal of Physical Chemistry B* **2003**, *107*, 5432(c) Lin, D. C.; Zhou, W. Z.; Guo, J.; He, H. Y.; Long, Y. C. *Journal of Physical Chemistry B* **2003**, *107*, 3789(d) White, C.; Ruiz-Salvador, A. R.; Lewis, D. W. *Angewandte Chemie-International Edition* **2004**, *43*, 469(e) Ruiz-Salvador, A. R.; Almora-Barrios, N.; Gomez, A.; Lewis, D. W. *Physical Chemistry Chemical Physics* **2007**, *9*, 521(f) Gomez-Hortiguela, L.; Perez-Pariente, J.; Cora, F. *Chemistry - A European Journal* **2009**, *15*, 1478

(14) (a) Gale, J. D. *Journal of the Chemical Society-Faraday Transactions* **1997**, *93*, 629(b) Gale, J. D.; Rohl, A. L. *Molecular Simulation* **2003**, *29*, 291.

(15) (a) Demuth, T.; Hafner, J.; Benco, L.; Toulhoat, H. *Journal of Physical Chemistry B* **2000**, *104*, 4593(b) Blasco, T.; Corma, A.; Diaz-Cabanas, M. J.; Rey, F.; Vidal-Moya, J. A.; Zicovich-Wilson, C. M. *Journal of Physical Chemistry B* **2002**, *106*, 2634(c) Gale, J. D. *Solid State Sciences* **2006**, *8*, 234(d) Oumi, Y.; Kanai, T.; Lu, B.; Sano, T.

Microporous and Mesoporous Materials **2007**, *101*, 127(e) Sun, K.; Fan, F.; Xia, H.; Feng, Z.; Li, W.-X.; Li, C. *Journal of Physical Chemistry C* **2008**, *112*, 16036.

(16) (a) Mellot-Draznieks, C.; Ferey, G. *Current Opinion in Solid State & Materials Science* **2003**, *7*, 13(b) Catlow, C. R. A.; Bell, R.; Cora, F.; Slater, B. In *Introduction to zeolite science and pratice 3 Revised edition, Studies in Surface Science and Catalysis*; J. Cejka, H. v. B., A. Corma, F. Schuth, Ed.; Elsevier: Amsterdam, 2007; Vol. 169.

(17) (a) Lewis, D. W.; Catlow, C. R. A.; Sankar, G.; Carr, S. W. *J. Phys. Chem.* **1995**, *99*, 2377(b) Wright, P. A.; Sayag, C.; Rey, F.; Lewis, D. W.; Gale, J. D.; Natarajan, S.; Thomas, J. M. *J. Chem. Soc. Faraday Trans.* **1995**, *91*, 3537(c) Bushuev, Y. G.; Sastre, G. *J. Phys. Chem. C* **2010**, *114*, 19157.

(18) (a) Ruiz-Salvador, A. R.; Lewis, D. W.; Rubayo-Soneira, J.; Rodriguez-Fuentes, G.; Sierra, L. R.; Catlow, C. R. A. *Journal of Physical Chemistry B* **1998**, *102*, 8417(b) Ruiz-Salvador, A. R.; Gomez, A.; Lewis, D. W.; Rodriguez-Fuentes, G.; Montero, L. *Physical Chemistry Chemical Physics* **1999**, *1*, 1679(c) Ruiz-Salvador, A. R.; Gómez, A.; Lewis, D. W.; Catlow, C. R. A.; Rodríguez-Albelo, L. M.; Montero, L.; Rodríguez-Fuentes, G. *Physical Chemistry Chemical Physics* **2000**, *2*, 1803.

(19) Sanders, M. J.; Leslie, M.; Catlow, C. R. A. *Journal of the Chemical Society-Chemical Communications* **1984**, 1271.

(20) Jackson, R. A.; Catlow, C. R. A. *Molec. Sim.* **1988**, *1*, 207.

(21) (a) Ewald, P. P. *Annalen der Physik* **1921**, *64*, 253(b) Tosi, M. P. *Soild State Phys.* **1964**, *16*, 1.

(22) Shanno, D. F. *Math. Comp.* **1970**, *24*, 647.

(23) Simons, J.; Joergensen, P.; Taylor, H.; Ozment, J. *Journal of Physical Chemistry* **1983**, *87*, 2745.

(24) (a) Ruiz-Salvador, A. R.; Sastre, G.; Lewis, D. W.; Catlow, C. R. A. *Journal of Materials Chemistry* **1996**, *6*, 1837(b) Henson, N. J.; Cheetham, A. K.; Gale, J. D. *Chemistry of Materials* **1996**, *8*, 664.

(25) (a) Chatterjee, A.; Vetrivel, R. *Journal of the Chemical Society-Faraday Transactions* **1995**, *91*, 4313(b) Chatterjee, A.; Vetrivel, R. *Journal of Molecular Catalysis a-Chemical* **1996**, *106*, 75.

(26) Kramer, G. J.; Vansanten, R. A.; Emeis, C. A.; Nowak, A. K. *Nature* **1993**, *363*, 529.

(27) Grau-Crespo, R.; Hamad, S.; Catlow, C. R. A.; de Leeuw, N. H. *Journal of Physics-Condensed Matter* **2007**, *19*, 256201.

(28) (a) Grau-Crespo, R.; de Leeuw, N. H.; Catlow, C. R. A. *Chemistry of Materials* **2004**, *16*, 1954(b) Benny, S.; Grau-Crespo, R.; De Leeuw, N. H. *Physical Chemistry Chemical Physics* **2009**, *11*, 808 (c) Grau-Crespo, R.; De Leeuw, N. H.; Hamad, S.; Waghmare, U. V. *Proceedings of the Royal Society a-Mathematical Physical and Engineering Sciences* **2011**, *467*, 1925.

(29) (a) Haider, S.; Grau-Crespo, R.; Devey, A. J.; de Leeuw, N. H. *Geochimica et Cosmochimica Acta* **2012**, *88*, 275(b) Seminovski, Y.; Palacios, P.; Wahnon, P.; Grau-Crespo, R. *Applied Physics Letters* **2012**, *100*, 102112.

(30) (a) Ruiz-Hernandez, S. E.; Grau-Crespo, R.; Ruiz-Salvador, A. R.; De Leeuw, N. H. *Geochimica et Cosmochimica Acta* **2010**, *74*, 1320(b) Wang, Q.; Grau-Crespo, R.; De Leeuw, N. H. *Journal of Physical Chemistry B* **2011**, *115*, 13854.

(31) (a) Grau-Crespo, R.; Smith, K. C.; Fisher, T. S.; De Leeuw, N. H.; Waghmare, U. V. *Physical Review B* **2009**, *80*, 174117 (b) Smith, K. C.; Fisher, T. S.; Waghmare, U. V.; Grau-Crespo, R. *Physical Review B* **2010**, *82*, 134109.

(32) Sastre, G.; Fornes, V.; Corma, A. *Journal of Physical Chemistry B* **2002**, *106*, 701.

(33) (a) Shantz, D. F.; Fild, C.; Koller, H.; Lobo, R. F. *J. Phys. Chem. B* **1999**, *103*, 10858(b) Gomez-Hortiguela, L.; Pinar, A. B.; F., C.; Perez-Pariente, J. *Chem. Commun.* **2010**, *46*, 2073.